QRB DISCOVERY
journals.cambridge.org/qrb

PERSPECTIVE

Electron flow through biological molecules: does hole hopping protect proteins from oxidative damage?

Jay R. Winkler and Harry B. Gray*

Beckman Institute, California Institute of Technology, Pasadena, CA 91125, USA

Quarterly Reviews of Biophysics (2015), **48(4)**, pages 411–420 doi:10.1017/S0033583515000062

Abstract. Biological electron transfers often occur between metal-containing cofactors that are separated by very large molecular distances. Employing photosensitizer-modified iron and copper proteins, we have shown that single-step electron tunneling can occur on nanosecond to microsecond timescales at distances between 15 and 20 Å. We also have shown that charge transport can occur over even longer distances by hole hopping (multistep tunneling) through intervening tyrosines and tryptophans. In this perspective, we advance the hypothesis that such hole hopping through Tyr/Trp chains could protect oxygenase, dioxygenase, and peroxidase enzymes from oxidative damage. In support of this view, by examining the structures of P450 (CYP102A) and 2OG-Fe (TauD) enzymes, we have identified candidate Tyr/Trp chains that could transfer holes from uncoupled high-potential intermediates to reductants in contact with protein surface sites.

Key words: electron transfer, protein radical, hole hopping, azurin, cytochrome P450.

Background

Many vital biological transformations involve the incorporation of one (monooxygenases) or two (dioxygenases) O-atoms from molecular oxygen into organic substrates. Enzymes that utilize oxygen must coordinate the delivery of four protons and four electrons to O_2 in order to prevent the formation of harmful molecular oxidants (O_2^-, $HO_2^•$ H_2O_2, and $HO^•$), collectively known as reactive oxygen species (ROS). It is our view that the risks posed by reactive intermediates are so great that oxygen-utilizing enzymes have protection mechanisms to help them avoid inactivation when the primary electron/proton transfer mechanism is disrupted.

The mechanism of O_2 reduction by cytochrome *c* oxidase illustrates some of the challenges facing these enzymes (Wikström, 2012; Yu *et al.* 2011, 2012). Reaction of the fully four-electron reduced enzyme ($Cu_A^{II,I}$, Fe^{II}-heme *a*, Fe^{II}-heme a_3, and Cu_B^{I}) with O_2 generates an intermediate designated as P_R. When the two-electron reduced, mixed valence enzyme ($Cu_A^{II,II}$, Fe^{III}-heme *a*, Fe^{II}-heme a_3, and Cu_B^{I}) reacts with O_2, the P_M intermediate is formed. The O–O bond has been cleaved in both P_R and P_M to produce $Fe^{IV}(O)$-heme a_3 and Cu_B^{II} in the binuclear site. The difference between P_R and P_M is in the source of the fourth electron: P_M is thought to have a Tyr^{244} radical (bovine numbering), whereas the fourth electron in P_R is provided by Fe^{II}-heme *a*. When P_M is prepared using H_2O_2, the hole on $(TyrO^•)^{244}$ is believed to migrate through $(Trp^{•+})^{236}$ to $(TyrO^•)^{129}$; the latter residue is suggested to participate in proton pumping (Yu *et al.* 2012). The key point is that Tyr^{244} is available to fill the gap when the fourth electron required for O_2 reduction cannot be supplied by Fe^{II}-heme *a* (Wikström, 2012; Yu *et al.* 2012).

In many oxygenases, including the cytochromes P450 (P450) and the 2-oxo-glutarate-dependent nonheme iron oxygenases (2OG-Fe), the four electrons required for O_2 reduction have different origins (Fig. 1). Typically, two electrons are delivered from a reductase (P450) or co-substrate (2OG), and the remaining two electrons are provided by the organic substrate (Denisov *et al.* 2005; Hausinger, 2004;

* Author for correspondence: Beckman Institute, MC 139-74, California Institute of Technology, 1200 E. California Boulevard, Pasadena, CA 91125, USA. Tel: +626-395-6500; Fax: +626-449-4159; Email: hbgray@caltech.edu

© Cambridge University Press 2015. This is an Open Access article, distributed under the terms of the Creative Commons Attribution licence (http://creativecommons.org/licenses/by/3.0/), which permits unrestricted re-use, distribution, and reproduction in any medium, provided the original work is properly cited.

https://doi.org/10.1017/S0033583515000062 Published online by Cambridge University Press

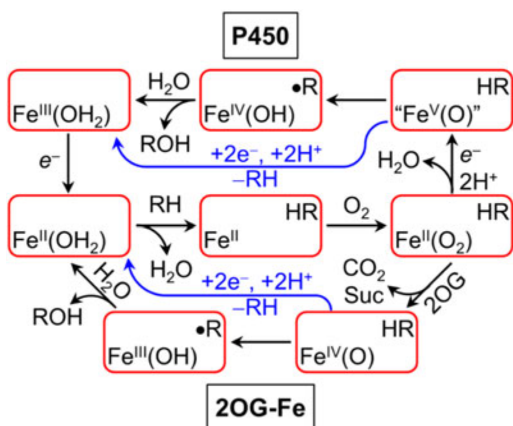

Fig. 1. Schematic representation of the catalytic mechanisms of P450 and 2OG-Fe oxygenases: RH, substrate; 2OG, 2-oxoglutarate; Suc, succinate. Black arrows indicate the functional substrate hydroxylation pathways. Blue arrows indicate oxidase uncoupling pathways.

Whitehouse *et al.* 2012). In the consensus mechanism for iron oxygenases, the first two electrons induce O–O bond cleavage, producing a powerfully oxidizing ferryl species. The ferryl complex abstracts a hydrogen atom from the substrate and $HO^{\bullet}$ rebound leads to hydroxylated product (Denisov *et al.* 2005; Hausinger, 2004; Whitehouse *et al.* 2012). For enzymes with broad substrate specificities, or when operating in the presence of xenobiotic compounds, the fidelity of substrate oxidation is less than 100%, with potentially damaging consequences (Chen *et al.* 2008; De Matteis *et al.* 2012; Denisov *et al.* 2007*a*; Grinkova *et al.* 2013; Saban *et al.* 2011; Staudt *et al.* 1974). This circumstance is manifested as an increased molar ratio of O_2 consumption to substrate hydroxylation (uncoupling). We think it likely that organisms have evolved protection mechanisms to guard against deactivation of oxygenase enzymes in the event of uncoupled O_2 consumption. In particular, we suggest that radical transfer pathways are employed to deliver strongly oxidizing holes (E°∼1 V *versus* NHE) from ferryl complexes in active sites to less fragile regions of oxygenases.

In this perspective, we will advance the hypothesis that there are potentially protective radical chains in P450 and 2OG-Fe; but first we will review what we know about the factors controlling hopping through aromatic amino acids in multistep electron tunneling constructs designed in azurin, a prototypal cupredoxin.

Radical transfer pathways in azurin

Azurin is a robust cupredoxin (128 residues) that is amenable to site-directed mutagenesis and surface-labeling with photosensitizers (Farver & Pecht, 2011; Gray & Winkler, 2010; Reece & Nocera, 2009; Wilson *et al.* 2013). Oxidized radicals of Trp and Tyr are substantially stronger acids than their neutral precursors (Trp, $pK_a > 14$; $Trp^{\bullet +}$, $pK_a = 4$; TyrOH, $pK_a = 10$; $TyrOH^{\bullet +}$, $pK_a = -1$) (Aubert *et al.* 2000; Bonin *et al.* 2010; Costentin *et al.* 2009; Harriman, 1987; Jovanic *et al.* 1986); management of the acidic proton is a critically important factor controlling radical formation with these amino acids. Proton management is particularly challenging for buried amino acids and, thus far, we have not succeeded in detecting buried Trp or Tyr radicals as electron transfer (ET) intermediates. Our kinetics data indicate that surface exposed $Trp^{\bullet +}$ and $NO_2TyrO^{\bullet}$ radicals can, in appropriate constructs, accelerate Cu^I oxidation by distant Re- and Ru-diimine complexes (Shih *et al.* 2008; Warren *et al.* 2013*a*).

Multistep ET through Trp and Tyr radicals in azurin

We have used *Pseudomonas aeruginosa* azurin as a test bed for mechanistic investigations of Trp and Tyr radical formation in protein ET reactions (Blanco-Rodriguez *et al.* 2011; Shih *et al.* 2008; Takematsu *et al.* 2013; Warren *et al.* 2012, 2013*a*). Our initial investigation revealed that Cu^I oxidation by a photoexcited Re^I–diimine complex ($Re^I(CO)_3$(4,7-dimethyl-1,10-phenanthroline)) covalently bound at His^{124} on a $His^{124}Gly^{123}Trp^{122}Met^{121}$ *β*-strand ($ReHis^{124}Trp^{122}Cu^I$-azurin) occurs in a few nanoseconds, fully two orders of magnitude faster than documented for single-step electron tunneling at a 19-Å donor–acceptor distance, owing to a two-step hopping mechanism involving a $Trp^{\bullet +}$ radical intermediate (Shih *et al.* 2008).

Our work on multistep ET in sensitizer-modified azurin is informed by semiclassical ET theory (Marcus & Sutin, 1985). Given a particular spatial arrangement of redox cofactors, we can predict driving-force dependences of the relative time constants for single-step ($\tau_{ss} = 1/k_{ss}$) and multistep (τ_{hop}) electron transport (Warren *et al.* 2012). Alternatively, given the redox and reorganization energetics, we can predict the hopping propensity for different cofactor arrangements (Warren *et al.* 2013*a*). We considered three Ru(2,2′-bipyridine)$_2$(imidazole)(His^X)-labeled azurins ($RuHis^{107}$, $RuHis^{124}$, and $RuHis^{126}$) and examined the hopping advantage (τ_{ss}/τ_{hop}) for a protein with a generalized intermediate (Int) situated between a diimine-Ru^{III} oxidant and Cu^I (Warren *et al.* 2013*a*). In all cases, the greatest hopping advantage occurs in systems where the Int–Ru^{III} distance is up to 5 Å shorter than the Int–Cu^I distance. The hopping advantage increases as systems orient nearer a linear Donor–Int–Acceptor configuration, owing to minimized intermediate tunneling distances. The smallest predicted hopping advantage is in $RuHis^{124}$ azurin, which has the shortest Ru–Cu distance of the three proteins. The hopping advantage is nearly lost as $\Delta G°$ for the first step ($Ru^{III} \leftarrow$ Int) rises above +0.15 eV. Isoergic initial steps provide a wide distribution of arrangements, where advantages as great as 10^4 are possible (for a fixed donor–acceptor distance of 23.7 or 25.4 Å). A slightly exergonic Int → Ru^{III} step

https://doi.org/10.1017/S0033583515000062 Published online by Cambridge University Press

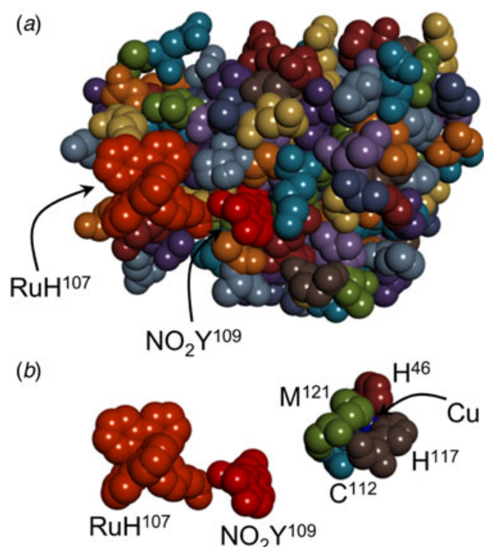

Fig. 2. (*a*) Space-filling structural model of $RuHis^{107}NO_2TyrOH^{109}$Cu-azurin. (*b*) Space filling models of the residues comprising the hole-hopping pathway from Cu to $RuHis^{107}$.

provides an even larger distribution of arrangements for productive hopping, which will be the case as long as the driving force for the first step is not more favorable than that for overall transfer.

We tested these predictions experimentally in three Ru–His-labeled azurins using nitrotyrosinate (NO_2TyrO^-) as a redox intermediate ($RuHis^{107}(NO_2TyrOH)^{109}$; $RuHis^{124}(NO_2TyrOH)^{122}$; and $RuHis^{126-}(NO_2TyrOH)^{122}$; $E°'(NO_2TyrO^{\bullet/-}) \approx 1.02$ V *versus* NHE) (Fig. 2) (Warren *et al.* 2013*a*). The first two systems have cofactor placements that are close to the predicted optimum; the last system has a larger first-step distance, which is predicted to decrease the hopping advantage. The phenol pK_a of 3-nitrotyrosine (7.2) permitted us to work at near-neutral pH, rather than high pH (>10) required for hopping with tyrosinate. ET via nitrotyrosinate avoids the complexities associated with the proton-coupled redox reactions of tyrosine. We found specific rates of Cu^I oxidation more than 10 times greater than those of single-step ET in the corresponding azurins lacking NO_2TyrOH, confirming that NO_2TyrO^- accelerates long-range ET. The results are in excellent agreement with hopping maps developed using semiclassical ET theory and parameters derived from our body of protein ET measurements (Gray & Winkler, 2010; Warren *et al.* 2012, 2013*a*).

Potential radical transfer pathways in iron oxygenases

The cytochromes P450 are members of a superfamily of heme oxygenases that perform two broad functional roles: xenobiotic metabolism and biosynthesis (Denisov *et al.* 2005; Johnson & Stout, 2013; Nebert *et al.* 2013; Orr *et al.* 2012; Whitehouse *et al.* 2012). The oxygenation chemistry catalyzed by some P450 enzymes is tightly coupled to substrate hydroxylation: one mole of product is produced for each mole of O_2 consumed. In many enzymes, however, particularly the eukaryotic proteins with broad substrate specificities, hydroxylation is much less efficiently coupled to O_2 consumption (frequently less than 10%) (Denisov *et al.* 2007*a*; Grinkova *et al.* 2013; Staudt *et al.* 1974). When the enzyme does not transfer an O-atom to substrate, it can produce ROS (O_2^-, H_2O_2) or a second H_2O molecule (Puntarulo & Cederbaum, 1998). The production of ROS can lead to rapid degradation of the enzyme and other harmful chemistry. In the case of oxidase chemistry (formation of $2H_2O$ from O_2), two reducing equivalents must be delivered by sources other than the substrate. When a CYP enzyme binds a refractory substrate, ferryl formation is likely to proceed, but substrate hydroxylation is inhibited. Under these circumstances, chains of redox-active Tyr, Trp, Cys, and/or Met residues can direct the oxidizing hole to the protein periphery where it can react with intracellular antioxidants such as glutathione.

Enzymes from the 2OG-Fe superfamily use 2-oxoglutarate as a 2-electron donating co-substrate, Fe^{2+} as a cofactor, and O_2 to effect the hydroxylation of organic substrates (Fig. 1). The 2OG-Fe enzymes exhibit a wide array of biological functions including collagen biosynthesis, lysyl hydroxylation of RNA splicing proteins, DNA repair, RNA modification, chromatin regulation, epidermal growth factor-like domain modification, hypoxia sensing, and fatty acid metabolism (Mantri *et al.* 2012; Rose *et al.* 2011). The 2OG-Fe oxygenase enzymes have conserved double-stranded *β*-helix folds with octahedral Fe-binding sites with the HXD/E…H triad providing two His imidazole ligands and one monodentate carboxylate ligand. The remaining three coordination sites in the resting enzyme are occupied by O-donors from 2OG and a water ligand.

Several 2OG-Fe enzymes have been reported to undergo autocatalyzed oxidative modifications of aromatic amino acids. In the taurine-2OG dioxygenase that catalyzes the conversion of taurine to bisulfite, EPR data indicate the transient formation of a Tyr^{73}-based radical that converts to an Fe^{III}-catecholate (Mantri *et al.* 2012). In 2,4-dichlorophenoxyacetate oxygenase (TfdA) and factor-inhibiting hypoxia-inducible factor (FIH) there is evidence for Trp hydroxylation when substrate is unavailable (Mantri *et al.* 2012). These aromatic amino acid oxidations lead to inactivation of the enzyme. As with P450, we suggest that radical chains of Trp, Tyr, Cys, and/or Met residues in 2OG-Fe hydroxylases protect the enzymes from damage in the event of slow or unsuccessful substrate hydroxylation by diverting the powerfully oxidizing hole from $Fe^{IV}(O)$ to the protein surface, where it can react with intracellular reductants (e.g. glutathione). This diversion of oxidizing

https://doi.org/10.1017/S0033583515000062 Published online by Cambridge University Press

equivalents would extend the functional lifetime of an enzyme.

When considering the many remarkable transformations catalyzed by natural enzymes, it is easy to be left with the impression that these macromolecules are perfect catalysts that, after millions of years of tinkering, have solved the riddle of simultaneously maximizing speed, selectivity, and specificity. Upon closer inspection, however, heme and nonheme oxygenases are far from perfect catalysts, yet manage to accomplish their primary functions. Indeed, in many oxygenases, the coupling between oxygen consumption and substrate hydroxylation is extremely low. The most abundant P450 in human liver, CYP3A4, is a case in point (Denisov *et al.* 2007*b*; Grinkova *et al.* 2013). For enzyme incorporated into nanodiscs (Grinkova *et al.* 2010), the coupling of substrate hydroxylation to NADH consumption was ≤16% for testosterone as a substrate, ≤10% for bromocriptine, and 2% for tamoxifen (Grinkova *et al.* 2013). It is fair to say that, although the primary CYP3A4 function may be substrate hydroxylation, the primary enzyme activity is distributed more or less equally between H_2O_2 and H_2O production (Grinkova *et al.* 2013). Indeed, it would not be inaccurate to characterize CYP3A4 as a flawed oxidase that occasionally oxygenates organic substrates. More importantly, unless the enzyme was protected from damage in the event of uncoupled turnover, CYP3A4 would function not as a catalyst but as a stoichiometric reagent. A similar situation exists for uncoupled turnover in the 2OG-Fe enzymes.

The active sites of heme and nonheme oxygenases often are deeply buried within a polypeptide matrix. Consequently, powerfully oxidizing active site holes cannot efficiently migrate in single-step tunneling reactions to the enzyme surface for reduction by external reagents (Winkler & Gray, 2014*a*, *b*). We have shown that multistep tunneling reactions can be hundreds to thousands of times faster than their single-step counterparts (Shih *et al.* 2008; Warren *et al.* 2012, 2013*a*, *b*). Radical transfer pathways composed of Tyr, Trp, Cys, and Met residues are ideally suited to deliver active-site oxygenase holes to enzyme surfaces when reaction with substrate is disrupted.

A biologically useful Fe-oxygenase protection mechanism requires that a fine balance be struck between substrate reaction and hole migration to the surface. Overly efficient hole migration would lower enzyme hydroxylation activity, while a sluggish pathway would be ineffective at protecting the enzyme. Active-site hole scavenging in P450 by the natural reductase may be possible, but the timing of this reaction would be extremely variable, owing to fluctuations in reductase concentration. In the 2OG-Fe enzymes, there is no reductase that could protect the enzyme. An intraprotein radical transfer mechanism can be tuned to provide the proper balance between enzyme protection and substrate reaction. We suggest that the first step in the hole-migration pathway is the critical determinant of ferryl survival time. Once a radical forms on the first residue in the pathway (the gateway residue), further migration to the surface is rapid. In the potential pathways that we have identified, the distance from the active site to the first pathway residue is often longer than subsequent steps. In addition to the longer distance, proton coupling and enzyme conformational changes could contribute to limiting the rate of the first step in the transfer chain.

CYP102A1

CYP102A1 from *Bacillus megaterium* (also known as P450 BM3) is a rare example of a bacterial Class II cytochrome P450 enzyme in which both reductase and heme domains are contained within a single polypeptide chain (Miura & Fulco, 1974; Narhi & Fulco, 1986). The enzyme catalyzes the remarkably rapid hydroxylation of long-chain fatty acids using NAD(P)H and O_2, without the presence of any other proteins or cofactors (Narhi & Fulco, 1986). The full-length enzyme ($CYP102A1_{HR}$) has been expressed in *Escherichia coli*, as have independent heme ($CYP102A1_H$) and reductase ($CYP102A1_R$) domains (Boddupalli *et al.* 1990, 1992; Li *et al.* 1991*a*; Narhi *et al.* 1988; Oster *et al.* 1991). The individual domains, as well as an assembly between the heme domain and a flavin-containing reductase domain, have been structurally characterized (Girvan *et al.* 2007; Sevrioukova *et al.* 2000; Warman *et al.* 2005). The soluble, 119 kDa $CYP102A1_H$ enzyme serves as a convenient model system for the more complex membrane-bound enzyme assemblies (Whitehouse *et al.* 2012).

Uncoupled substrate, O_2, and NAD(P)H consumption in P450 catalysis is a well-recognized and relatively common phenomenon (De Matteis *et al.* 2002, 2012; Denisov *et al.* 2007*a*; Grinkova *et al.* 2013; Puntarulo & Cederbaum, 1998; Staudt *et al.* 1974). If two reducing equivalents are not delivered to O_2 by the substrate, then alternative sources are necessary to avoid ROS production and/or enzyme degradation. In some cases, the extra equivalents can be delivered by NAD(P)H, leading to NAD(P)H : O_2 molar consumption ratios greater than 1 (De Matteis *et al.* 2012). Exogenous reductants such as bilirubin and uroporphyrinogen have been shown to contribute reducing equivalents during NAD(P)H/O_2 CYP102A1 turnover in the presence of halogenated (perfluorolaurate) substrates (De Matteis *et al.* 2012). Although it is possible that an active site hole could tunnel to the protein surface in a single step, a multistep radical transfer mechanism would be far more efficient. There are two attractive radical transfer pathways from the CYP102A1 heme to the protein surface (Fig. 3) (Girvan *et al.* 2007). Pathway I is comprised of heme–Trp^{96}–Trp^{90}–Tyr^{334}; pathway II is heme–Cys^{156}–Tyr^{115}–Met^{112}–Tyr^{305}.

https://doi.org/10.1017/S0033583515000062 Published online by Cambridge University Press

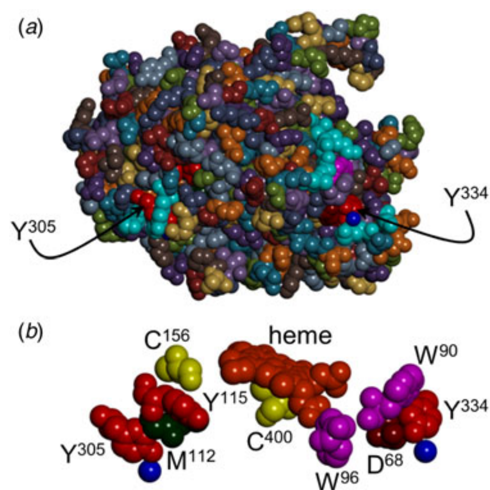

Fig. 3. (*a*) Space-filling structural model of the heme domain of CYP102A1 (PDB #2IJ2) highlighting the surface locations of terminal residues in pathways I (Tyr^{334}) and II (Tyr^{305}). (*b*) Space-filling model of the residues comprising CYP102A1 radical transfer pathways I and II. Blue spheres represent structurally resolved water molecules.

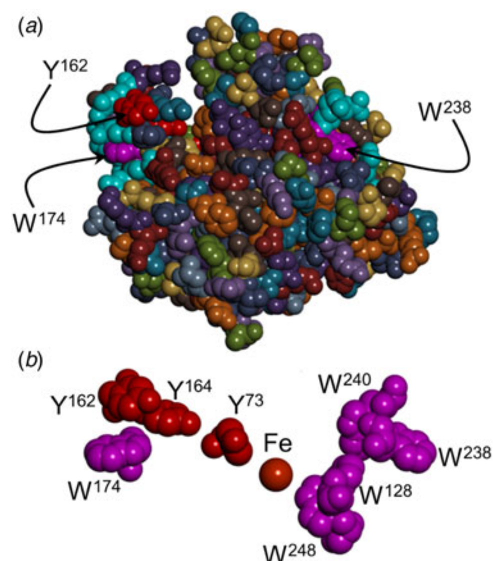

Fig. 4. (*a*) Space-filling structural model of *E. coli* TauD (PDB #1OS7) highlighting the surface locations of terminal residues in postulated radical transfer pathways (Trp^{238}, Trp^{174}, and Tyr^{162}). (*b*) Space-filling model of the residues comprising TauD radical transfer pathways.

CYP102A1 radical transfer pathway I

The shortest direct distance between aromatic atoms of CYP102A1 Trp^{96} and the heme is 7.3 Å and $Trp(N\varepsilon)^{96}$ is hydrogen bonded to the heme propionate (Girvan *et al.* 2007). Sequence alignment (UniProtKB) in the P450 family suggests that Trp is conserved at this position in >75% of the members of this group. Interestingly, of the 698 sequences with Trp at this position, all but 5 derive from eukaryotic sources, whereas about half of the proteins with His at this position derive from bacterial or archaeal sources. In this regard, it is noteworthy that archaeal CYP119 does not have a Trp residue at this site and is the only P450 in which Cmpd-1 has been characterized (Park *et al.* 2002; Rittle & Green, 2010). The strong conservation of the Trp^{96} residue has been noted previously (Munro *et al.* 1994). To the best of our knowledge, no role other than structural has been reported for this highly conserved Trp residue in P450 (Whitehouse *et al.* 2012).

We suggest that Trp^{96} is the gateway residue for hole transfer from the heme to the protein surface during uncoupled turnover. Studies of the reactions of substrate-free $P450_{cam}$ (CYP101) with peracids revealed that a second intermediate (Cmpd-ES) forms as a result of ET from a Tyr residue to Cmpd-1 (Schünemann *et al.* 2004; Spolitak *et al.* 2005, 2006, 2008). A Cmpd-ES intermediate has been detected in CYP102A1 and Trp^{96} has been implicated as one of the residues hosting the oxidized radical (Raner *et al.* 2006). Addition of NADPH to Cmpd-ES of the $CYP102_{HR}$ holoenzyme regenerates the ferric resting state; and formation of these radicals may play a protective role during uncoupled P450 catalysis (Spolitak *et al.* 2006). A combined computational/experimental investigation of CYP102A1 implicated buried Trp^{96}, Trp^{90}, His^{92}, and Tyr^{334} residues as components of an ET pathway that could deliver reducing equivalents to Cmpd-1 from the protein surface (Vidal-Limon *et al.* 2013). The shortest aromatic contacts in this chain are: Trp^{96}–Trp^{90}, 8.4 Å; Trp^{90}–Tyr^{334}, 4.4 Å (Girvan *et al.* 2007). The environment around Tyr^{334} appears well-suited for radical formation: the phenol hydroxyl group is hydrogen-bonded to both a carboxylate (Asp^{68}) and a water molecule (HOH^{1215}).

Our prior studies of P450 ET reactions are consistent with involvement of Trp^{96} in a radical transfer pathway to the heme (Ener *et al.* 2010). We have found that $Ru^{II}(bpy)_2(phen^{\bullet-}–Cys^{97})$ can deliver an electron across 24 Å to the Fe^{III}-heme in 20 µs, and $Ru^{III}(bpy)_2(phen–Cys^{97})CYP102A1_H$ can oxidize the heme to a porphyrin radical in under 2 µs (Ener *et al.* 2010). The latter reaction is particularly rapid given the low driving force (<200 meV) expected for the transformation. We have prepared a Trp^{96}His mutant and found that $Ru^{III}(bpy)_2(phen–Cys^{97})(His^{96})CYP102A1_H$ does not promote photochemical heme oxidation to Cmpd-2. Electron transfer to the Fe^{III}-heme from $Ru^{II}(bpy)_2(phen^{\bullet-}–Cys^{97})(His^{96})$, however, is unaffected by the Trp^{96}His mutation.

CYP102A1 radical transfer pathway II

The second potential radical transfer pathway in CYP102A1, heme–Cys^{156}–Tyr^{115}–Met^{112}–Tyr^{305}, does not appear as favorable as pathway I, due largely to a long distance between the heme and the first step in the path. The distance from $Cys(S\gamma)^{156}$ to the closest heme aromatic

https://doi.org/10.1017/S0033583515000062 Published online by Cambridge University Press

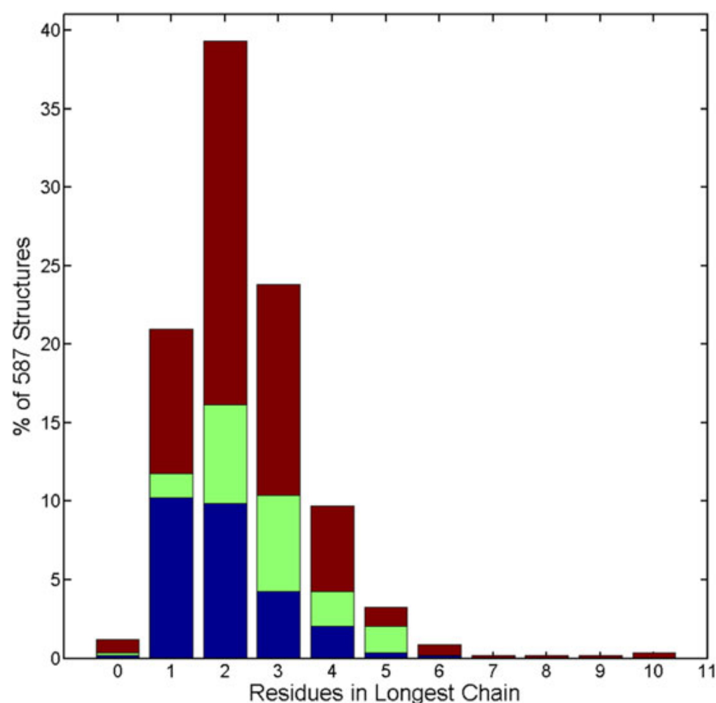

Fig. 5. Distributions of radical transfer chain lengths among structurally characterized oxidoreductases from enzyme sub-classes EC 1.11 (peroxidases, blue), 1.13 (oxygenases, green), and 1.14 (dioxygenases, red). Radical transfer chains are defined to be composed of Tyr, Trp, heme, Fe, and Cu residues. Tyr residues were included only if a carboxylate (Asp, Glu) oxygen atom, an imidazole (His) nitrogen atom, or a water molecule was within 4 Å of the Tyr hydroxyl oxygen atom.

carbon atom (10.8 Å) is slightly longer than the shortest aromatic–aromatic contact between the heme and Tyr^{115} (10.2 Å). If a radical is formed on Tyr^{115}, then hole transport to the surface Tyr^{305} via $Met(S\delta)^{112}$ could provide a secondary protection route.

Potential radical transfer pathways in 2OG-Fe oxygenases

TauD

The 2-oxoglutarate nonheme iron oxygenases catalyze substrate hydroxylation reactions in a fashion that is reminiscent of the cytochromes P450, but with some critical distinctions (Fig. 1). The consensus mechanism for catalysis involves Fe^{2+} binding to the apo-enzyme followed by 2OG incorporation. Substrate binding induces loss of the water ligand from Fe^{2+}, creating a vacant coordination site for O_2 binding. Oxidation of 2OG produces CO_2, succinate, and an $Fe^{IV}(O)$ center that is thought to hydroxylate substrate via the usual H-atom abstraction, hydroxyl rebound cycle (Mantri *et al.* 2012; Rose *et al.* 2011). The 2OG-Fe hydroxylases differ from the P450 enzymes in that substrate hydroxylation proceeds from the $Fe^{IV}(O)$ oxidation level (equivalent to P450 Cmpd-2). The *E. coli* 2OG-Fe enzyme TauD is synthesized under conditions of sulfur deprivation (Hausinger, 2004); large quantities of TauD have been prepared by over expression in *E. coli* BL21(DE3) (pME4141) cells (Eichhorn *et al.* 1997; Ryle *et al.* 1999). The enzyme catalyzes the hydroxylation of taurine (2-aminoethanesulfonate), producing an unstable species that decomposes into sulfite and aminoacetaldehyde (Hausinger, 2004). In the absence of taurine, the enzyme will slowly consume O_2 and become inactivated: protein analysis indicates hydroxylation of Tyr^{73} (Koehntop *et al.* 2006; Ryle *et al.* 2003). Although with deuterated substrates coupling between oxygen consumption and substrate hydroxylation is diminished, 2OG oxidation is not, suggesting that $Fe^{IV}(O)$ continues to be formed in the presence of refractory substrates; and bis-Tris buffer, a potential reducing agent, decreases coupling between O_2 activation and C–H hydroxylation (McCusker & Klinman, 2009). We suggest that when $Fe^{IV}(O)$ is unable to effect substrate hydroxylation, the oxidizing hole is directed to the protein surface where it can be reduced by external reagents.

TauD radical transfer pathways

We have identified two possible radical transfer pathways in the structure of TauD: the most attractive pathway from Fe to the surface has four Trp residues: Fe–Trp^{248}–Trp^{128}–Trp^{240}–Trp^{238}; relevant distances are: Fe–Trp^{248}, 4.8 Å; Trp^{248}–Trp^{128}, 3.1 Å; Trp^{128}–Trp^{240}, 3.7 Å; Trp^{240}–Trp^{238}, 3.7 Å (Fig. 4) (O'Brien *et al.* 2003). The structure of this

https://doi.org/10.1017/S0033583515000062 Published online by Cambridge University Press

Trp chain compares favorably to that identified in *E. coli* DNA photolyase (4–5 Å separations) (Byrdin *et al.* 2003; Lukacs *et al.* 2006). The photolyase chain has just three Trp residues, and hole migration from $FADH^{\bullet *}$ to Trp^{306} at the protein surface is complete in less than 10 ns (Byrdin *et al.* 2003; Lukacs *et al.* 2006). We anticipate that a hole injected by Fe^{IV}(O)-TauD into Trp^{248} should migrate to Trp^{238} at the surface in less than 1 µs. A secondary radical transfer pathway in TauD [Fe–Tyr^{73}–Tyr^{164}–(Trp^{174}, Tyr^{162})] is of particular interest because hydroxylated Tyr^{73} has been found during turnover in the absence of taurine (Koehntop *et al.* 2006; Ryle *et al.* 2003). Both Trp^{174} and Tyr^{162} are well-exposed at the enzyme surface and both (or just one) of these residues could be involved in a radical transfer pathway. Relevant distances are: Fe–Tyr^{73}, 6.5 Å; Tyr^{73}–Tyr^{164}, 5.0 Å; Tyr^{164}–Trp^{174}, 4.2 Å; Tyr^{164}–Tyr^{162}, 7.6 Å; Trp^{174}–Tyr^{162}, 8.8 Å (O'Brien *et al.* 2003).

Outlook

Functional radical transfer pathways have been identified in several enzymes, including ribonucleotide reductase (Argirevic *et al.* 2012; Holder *et al.* 2012; Offenbacher *et al.* 2013*a*, *b*; Sjöberg, 1997; Stubbe & van der Donk, 1998; Stubbe *et al.* 2003; Worsdorfer *et al.* 2013; Yokoyama *et al.* 2011), photosystem II (Boussac *et al.* 2013; Keough *et al.* 2013; Sjoholm *et al.* 2012), DNA photolyase (Aubert *et al.* 1999, 2000; Byrdin *et al.* 2003; Kodali *et al.* 2009; Li *et al.* 1991*b*; Lukacs *et al.* 2006; Sancar, 2003; Taylor, 1994; Woiczikowski *et al.* 2011), and MauG (Davidson & Liu, 2012; Davidson & Wilmot, 2013; Geng *et al.* 2013; Yukl *et al.* 2013). If radical transfer pathways do indeed provide protection mechanisms for enzymes operating at high electrochemical potentials, then it is likely that they will be found in many more redox-active enzymes. A survey of oxidoreductases in the protein data bank reveals that nearly 80% of structurally characterized peroxidases, oxygenases, and dioxygenases (enzyme classes EC 1.11, 1.13, and 1.14; 587 structures with sequence identity less than 90%) contain chains of 2 or more redox-active residues (Tyr, Trp, heme, Fe, and Cu) separated by no more than 5 Å (Fig. 5). The fraction increases to almost 90% if the cutoff distance is increased to 8 Å. We think it very likely that hole hopping through these types of radical transfer chains greatly reduces the production of ROS that destroy enzymes and other molecules in living cells.

Acknowledgments

We thank Maraia Ener, Jeff Warren, Lionel Cheruzel, Kana Takematsu, and Oliver Shafaat for helpful discussions.

Financial support

Research reported in this publication was supported by The National Institute of Diabetes and Digestive and Kidney Diseases of the National Institutes of Health under award number R01DK019038 to HBG and JRW. The content is solely the responsibility of the authors and does not necessarily represent the official views of the National Institutes of Health. Additional support was provided by the Arnold and Mabel Beckman Foundation.

References

Argirevic, T., Riplinger, C., Stubbe, J., Neese, F. & Bennati, M. (2012). ENDOR spectroscopy and DFT calculations: evidence for the hydrogen-bond network within alpha 2 in the PCET of *E. coli* ribonucleotide reductase. *Journal of the American Chemical Society* **134**, 17661–17670.

Aubert, C., Mathis, P., Eker, A. P. M. & Brettel, K. (1999). Intraprotein electron transfer between tyrosine and tryptophan in DNA photolysase from *Anacystis nidulans*. *Proceedings of the National Academy of Sciences of the United States of America* **96**, 5423–5427.

Aubert, C., Vos, M. H., Mathis, P., Eker, A. P. M. & Brettel, K. (2000). Intraprotein radical transfer during photoactivation of DNA photolyase. *Nature* **405**, 586–590.

Blanco-Rodriguez, A. M., Di Bilio, A. J., Shih, C., Museth, A. K., Clark, I. P., Towrie, M., Cannizzo, A., Sudhamsu, J., Crane, B. R., Sykora, J., Winkler, J. R., Gray, H. B., Zalis, S. & Vlcek, A. (2011). Phototriggering electron flow through Re^{I}-modified *Pseudomonas aeruginosa* azurins. *Chemistry – A European Journal* **17**, 5350–5361.

Boddupalli, S. S., Estabrook, R. W. & Peterson, J. A. (1990). Fatty-acid monooxygenation by cytochrome-P-450BM-3. *Journal of Biological Chemistry* **265**, 4233–4239.

Boddupalli, S. S., Oster, T., Estabrook, R. W. & Peterson, J. A. (1992). Reconstitution of the fatty-acid hydroxylation function of cytochrome-P-450BM-3 utilizing its individual recombinant hemoprotein and flavoprotein domains. *Journal of Biological Chemistry* **267**, 10375–10380.

Bonin, J., Costentin, C., Louault, C., Robert, M., Routier, M. & Saveant, J. M. (2010). Intrinsic reactivity and driving force dependence in concerted proton-electron transfers to water illustrated by phenol oxidation. *Proceedings of the National Academy of Sciences of the United States of America* **107**, 3367–3372.

Boussac, A., Rappaport, F., Brettel, K. & Sugiura, M. (2013). Charge recombination in $S_nTyr_Z^{\bullet}Q_A^{-\bullet}$ radical pairs in D1 protein variants of photosystem II: long range electron transfer in the marcus inverted region. *Journal of Physical Chemistry B* **117**, 3308–3314.

Byrdin, M., Eker, A. P. M., Vos, M. H. & Brettel, K. (2003). Dissection of the triple tryptophan electron transfer chain in *Escherichia coli* DNA photolyase: Trp382 is the primary donor in photoactivation. *Proceedings of the National Academy of Sciences of the United States of America* **100**, 8676–8681.

Chen, Y. H., Comeaux, L. M., Herbst, R. W., Saban, E., Kennedy, D. C., Maroney, M. J. & Knapp, M. J. (2008). Coordination changes and auto-hydroxylation of FIH-1: uncoupled O_2-activation in a

https://doi.org/10.1017/S0033583515000062 Published online by Cambridge University Press

human hypoxia sensor. *Journal of Inorganic Biochemistry* **102**, 2120–2129.

Costentin, C., Louault, C., Robert, M. & Saveant, J. M. (2009). The electrochemical approach to concerted proton-electron transfers in the oxidation of phenols in water. *Proceedings of the National Academy of Sciences of the United States of America* **106**, 18143–18148.

Davidson, V. L. & Liu, A. M. (2012). Tryptophan tryptophylquinone biosynthesis: a radical approach to posttranslational modification. *Biochimica et Biophysica Acta – Proteins and Proteomics* **1824**, 1299–1305.

Davidson, V. L. & Wilmot, C. M. (2013). Posttranslational biosynthesis of the protein-derived cofactor tryptophan tryptophylquinone. *Annual Review of Biochemistry* **82**, 531–550.

De Matteis, F., Ballou, D. P., Coon, M. J., Estabrook, R. W. & Haines, D. C. (2012). Peroxidase-like activity of uncoupled cytochrome P450. Studies with bilirubin and toxicological implications of uncoupling. *Biochemical Pharmacology* **84**, 374–382.

De Matteis, F., Dawson, S. J., Pons, N. & Pipino, S. (2002). Bilirubin and uroporphyrinogen oxidation by induced cytochrome P4501A and cytochrome P4502B – role of polyhalogenated biphenyls of different configuration. *Biochemical Pharmacology* **63**, 615–624.

Denisov, I. G., Baas, B. J., Grinkova, Y. V. & Sligar, S. G. (2007*a*). Cooperativity in cytochrome P450 3A4 – Linkages in substrate binding, spin state, uncoupling, and product formation. *Journal of Biological Chemistry* **282**, 7066–7076.

Denisov, I. G., Grinkova, Y. V., McLean, M. A. & Sligar, S. G. (2007*b*). The one-electron autoxidation of human cytochrome p450 3A4. *Journal of Biological Chemistry* **282**, 26865–26873.

Denisov, I. G., Makris, T. M., Sligar, S. G. & Schlichting, I. (2005). Structure and chemistry of cytochrome P450. *Chemical Reviews* **105**, 2253–2277.

Eichhorn, E., van der Ploeg, J. R., Kertesz, M. A. & Leisinger, T. (1997). Characterization of α-Ketoglutarate-dependent taurine dioxygenase from *Escherichia coli*. *Journal of Biological Chemistry* **272**, 23031–23036.

Ener, M. E., Lee, Y. T., Winkler, J. R., Gray, H. B. & Cheruzel, L. (2010). Photooxidation of cytochrome P450-BM3. *Proceedings of the National Academy of Sciences of the United States of America* **107**, 18783–18786.

Farver, O. & Pecht, I. (2011). Electron transfer in blue copper proteins. *Coordination Chemistry Reviews* **255**, 757–773.

Geng, J. F., Dornevil, K., Davidson, V. L. & Liu, A. M. (2013). Tryptophan-mediated charge-resonance stabilization in the bis-Fe(IV) redox state of MauG. *Proceedings of the National Academy of Sciences of the United States of America* **110**, 9639–9644.

Girvan, H. M., Seward, H. E., Toogood, H. S., Cheesman, M. R., Leys, D. & Munro, A. W. (2007). Structural and spectroscopic characterization of P450BM3 mutants with unprecedented P450 heme iron ligand sets – new heme ligation states influence conformational equilibria in P450BM3. *Journal of Biological Chemistry* **282**, 564–572.

Gray, H. B. & Winkler, J. R. (2010). Electron flow through metalloproteins. *Biochimica Et Biophysica Acta – Bioenergetics* **1797**, 1563–1572.

Grinkova, Y. V., Denisov, I. G., McLean, M. A. & Sligar, S. G. (2013). Oxidase uncoupling in heme monooxygenases: human cytochrome P450 CYP3A4 in nanodiscs. *Biochemical and Biophysical Research Communications* **430**, 1223–1227.

Grinkova, Y. V., Denisov, I. G. & Sligar, S. G. (2010). Functional reconstitution of monomeric CYP3A4 with multiple cytochrome P450 reductase molecules in nanodiscs. *Biochemical and Biophysical Research Communications* **398**, 194–198.

Harriman, A. (1987). Further comments on the redox potentials of tryptophan and tyrosine. *Journal of Physical Chemistry* **91**, 6102–6104.

Hausinger, R. P. (2004). Fe(II)/alpha-ketoglutarate-dependent hydroxylases and related enzymes. *Critical Reviews in Biochemistry and Molecular Biology* **39**, 21–68.

Holder, P. G., Pizano, A. A., Anderson, B. L., Stubbe, J. & Nocera, D. G. (2012). Deciphering radical transport in the large subunit of class I ribonucleotide reductase. *Journal of the American Chemical Society* **134**, 1172–1180.

Johnson, E. F. & Stout, C. D. (2013). Structural diversity of eukaryotic membrane cytochrome P450s. *Journal of Biological Chemistry* **288**, 17082–17090.

Jovanic, S. V., Harriman, A. & Simic, M. G. (1986). Electron-transfer reactions of tryptophan and tyrosine derivatives. *Journal of Physical Chemistry* **90**, 1935–1939.

Keough, J. M., Zuniga, A. N., Jenson, D. L. & Barry, B. A. (2013). Redox control and hydrogen bonding networks: proton-coupled electron transfer reactions and tyrosine Z in the photosynthetic oxygen-evolving complex. *Journal of Physical Chemistry B* **117**, 1296–1307.

Kodali, G., Siddiqui, S. U. & Stanley, R. J. (2009). Charge redistribution in oxidized and semiquinone *E. coli* DNA photolyase upon photoexcitation: stark spectroscopy reveals a rationale for the position of Trp382. *Journal of the American Chemical Society* **131**, 4795–4807.

Koehntop, K. D., Marimanikkuppam, S., Ryle, M. J., Hausinger, R. P. & Que, L. (2006). Self-hydroxylation of taurine/alpha-ketoglutarate dioxygenase: evidence for more than one oxygen activation mechanism. *Journal of Biological Inorganic Chemistry* **11**, 63–72.

Li, H. Y., Darwish, K. & Poulos, T. L. (1991*a*). Characterization of recombinant *Bacillus megaterium* cytochrome-P-450BM-3 and its 2 functional domains. *Journal of Biological Chemistry* **266**, 11909–11914.

Li, Y. F., Heelis, P. F. & Sancar, A. (1991*b*). Active site of DNA photolyase: tryptophan-306 is the intrinsic hydrogen atom donor essential for flavin radical photoreduction and DNA repair in vitro. *Biochemistry* **30**, 6322–6329.

Lukacs, A., Eker, A. P. M., Byrdin, M., Villette, S., Pan, J., Brettel, K. & Vos, M. H. (2006). Role of the middle residue in the triple tryptophan electron transfer chain of DNA photolyase: ultrafast spectroscopy of a Trp→Phe mutant. *Journal of Physical Chemistry B* **110**, 15654–15658.

Mantri, M., Zhang, Z. H., McDonough, M. A. & Schofield, C. J. (2012). Autocatalysed oxidative modifications to 2-oxoglutarate dependent oxygenases. *FEBS Journal* **279**, 1563–1575.

Marcus, R. A. & Sutin, N. (1985). Electron transfers in chemistry and biology. *Biochimica et Biophysica Acta* **811**, 265–322.

McCusker, K. P. & Klinman, J. P. (2009). Modular behavior of tauD provides insight into the origin of specificity in alpha-ketoglutarate-dependent nonheme iron oxygenases. *Proceedings of the National Academy of Sciences of the United States of America* **106**, 19791–19795.

https://doi.org/10.1017/S0033583515000062 Published online by Cambridge University Press

Miura, Y. & Fulco, A. J. (1974). (Omega – 2) Hydroxylation of fatty-acids by a soluble system from *Bacillus megaterium*. *Journal of Biological Chemistry* **249**, 1880–1888.

Munro, A. W., Malarkey, K., McKnight, J., Thomson, A. J., Kelly, S. M., Price, N. C., Lindsay, J. G., Coggins, J. R. & Miles, J. S. (1994). The role of tryptophan-97 of cytochrome-P450-BM3 from *Bacillus megaterium* in catalytic function – evidence against the covalent-switching hypothesis of P450 electron-transfer. *Biochemical Journal* **303**, 423–428.

Narhi, L. O. & Fulco, A. J. (1986). Characterization of a catalytically self-sufficient 119,000-dalton cytochrome-P-450 monooxygenase induced by barbiturates in *Bacillus megaterium*. *Journal of Biological Chemistry* **261**, 7160–7169.

Narhi, L. O., Wen, L. P. & Fulco, A. J. (1988). Characterization of the protein expressed in *Escherichia coli* by a recombinant plasmid containing the *Bacillus megaterium* cytochrome-P-450BM-3 gene. *Molecular and Cellular Biochemistry* **79**, 63–71.

Nebert, D. W., Wikvall, K. & Miller, W. L. (2013). Human cytochromes P450 in health and disease. *Philosophical Transactions of the Royal Society B – Biological Sciences* **368** (1612), 20120431.

O'Brien, J. R., Schuller, D. J., Yang, V. S., Dillard, B. D. & Lanzilotta, W. N. (2003). Substrate-induced conformational changes in *Escherichia coli* taurine/α-ketoglutarate dioxygenase and insight into the oligomeric structure. *Biochemistry* **42**, 5547–5554.

Offenbacher, A. R., Burns, L. A., Sherrill, C. D. & Barry, B. A. (2013*a*). Redox-linked conformational control of proton-coupled electron transfer: Y122 in the ribonucleotide reductase β2 subunit. *Journal of Physical Chemistry B* **117**, 8457–8468.

Offenbacher, A. R., Minnihan, E. C., Stubbe, J. & Barry, B. A. (2013*b*). Redox-linked changes to the hydrogen-bonding network of ribonucleotide reductase β2. *Journal of the American Chemical Society* **135**, 6380–6383.

Orr, S. T. M., Ripp, S. L., Ballard, T. E., Henderson, J. L., Scott, D. O., Obach, R. S., Sun, H. & Kalgutkar, A. S. (2012). Mechanism-based inactivation (MBI) of cytochrome P450 enzymes: structure-activity relationships and discovery strategies to mitigate drug-drug interaction risks. *Journal of Medicinal Chemistry* **55**, 4896–4933.

Oster, T., Boddupalli, S. S. & Peterson, J. A. (1991). Expression, purification, and properties of the flavoprotein domain of cytochrome-P-450BM-3 – evidence for the importance of the amino-terminal region for FMN binding. *Journal of Biological Chemistry* **266**, 22718–22725.

Park, S.-Y., Yamane, K., Adachi, S.-I., Shiro, Y., Weiss, K. E., Maves, S. A. & Sligar, S. G. (2002). Thermophilic cytochrome P450 (CYP119) from *Sulfolobus solfataricus*: high resolution structure and functional properties. *Journal of Inorganic Biochemistry* **91**, 491–501.

Puntarulo, S. & Cederbaum, A. I. (1998). Production of reactive oxygen species by microsomes enriched in specific human cytochrome P450 enzymes. *Free Radical Biology and Medicine* **24**, 1324–1330.

Raner, G. M., Thompson, J. I., Haddy, A., Tangham, V., Bynum, N., Reddy, G. R., Ballou, D. P. & Dawson, J. H. (2006). Spectroscopic investigations of intermediates in the reaction of cytochrome P450(BM3)-F87G with surrogate oxygen atom donors. *Journal of Inorganic Biochemistry* **100**, 2045–2053.

Reece, S. Y. & Nocera, D. G. (2009). Proton-coupled electron transfer in biology: results from synergistic studies in natural and model systems. *Annual Review of Biochemistry*, **78**, 673–699.

Rittle, J. & Green, M. T. (2010). Cytochrome P450 compound I: capture, characterization, and C–H bond activation kinetics. *Science* **330**, 933–937.

Rose, N. R., McDonough, M. A., King, O. N. F., Kawamura, A. & Schofield, C. J. (2011). Inhibition of 2-oxoglutarate dependent oxygenases. *Chemical Society Reviews* **40**, 4364–4397.

Ryle, M. J., Liu, A., Muthukumaran, R. B., Ho, R. Y. N., Koehntop, K. D., McCracken, J., Que, L. & Hausinger, R. P. (2003). O-2- and alpha-ketoglutarate-dependent tyrosyl radical formation in TauD, an alpha-keto acid-dependent non-heme iron dioxygenase. *Biochemistry* **42**, 1854–1862.

Ryle, M. J., Padmakumar, R. & Hausinger, R. P. (1999). Stopped-flow kinetic analysis of *Escherichia coli* taurine/α-ketoglutarate dioxygenase: interactions with α-ketoglutarate, taurine, and oxygen†. *Biochemistry* **38**, 15278–15286.

Saban, E., Flagg, S. C. & Knapp, M. J. (2011). Uncoupled O_2-activation in the human HIF-asparaginyl hydroxylase, FIH, does not produce reactive oxygen species. *Journal of Inorganic Biochemistry* **105**, 630–636.

Sancar, A. (2003). Structure and function of DNA photolyase and cryptochrome blue-light photoreceptors. *Chemical Reviews* **103**, 2203–2238.

Schünemann, V., Lendzian, F., Jung, C., Contzen, J., Barra, A. L., Sligar, S. G. & Trautwein, A. X. (2004). Tyrosine radical formation in the reaction of wild type and mutant cytochrome P450cam with peroxy acids – a multifrequency EPR study of intermediates on the millisecond time scale. *Journal of Biological Chemistry* **279**, 10919–10930.

Sevrioukova, I. F., Immoos, C. E., Poulos, T. L. & Farmer, P. (2000). Electron transfer in the ruthenated heme domain of cytochrome P450BM-3. *Israel Journal of Chemistry* **40**, 47–53.

Shih, C., Museth, A. K., Abrahamsson, M., Blanco-Rodriguez, A. M., Di Bilio, A. J., Sudhamsu, J., Crane, B. R., Ronayne, K. L., Towrie, M., Vlcek, A., Richards, J. H., Winkler, J. R. & Gray, H. B. (2008). Tryptophan-accelerated electron flow through proteins. *Science* **320**, 1760–1762.

Sjöberg, B. M. (1997). Ribonucleotide reductases – a group of enzymes with different metallosites and a similar mechanism. *Structure and Bonding* **88**, 139–173.

Sjoholm, J., Styring, S., Havelius, K. G. V. & Ho, F. M. (2012). Visible light induction of an electron paramagnetic resonance split signal in photosystem II in the S-2 state reveals the importance of charges in the oxygen-evolving center during catalysis: a unifying model. *Biochemistry* **51**, 2054–2064.

Spolitak, T., Dawson, J. H. & Ballou, D. P. (2005). Reaction of ferric cytochrome P450cam with peracids – kinetic characterization of intermediates on the reaction pathway. *Journal of Biological Chemistry* **280**, 20300–20309.

Spolitak, T., Dawson, J. H. & Ballou, D. P. (2006). Rapid kinetics investigations of peracid oxidation of ferric cytochrome P450cam: nature and possible function of compound ES. *Journal of Inorganic Biochemistry* **100**, 2034–2044.

Spolitak, T., Dawson, J. H. & Ballou, D. P. (2008). Replacement of tyrosine residues by phenylalanine in cytochrome P450cam alters the formation of Cpd II-like species in reactions with artificial oxidants. *Journal of Biological Inorganic Chemistry* **13**, 599–611.

https://doi.org/10.1017/S0033583515000062 Published online by Cambridge University Press

Staudt, H., Lichtenb, F. & Ullrich, V. (1974). Role of NADH in uncoupled microsomal monoxygenations. *European Journal of Biochemistry* **46**, 99–106.

Stubbe, J., Nocera, D. G., Yee, C. S. & Chang, M. C. Y. (2003). Radical initiation in the class I ribonucleotide reductase: long-range proton-coupled electron transfer? *Chemical Reviews* **103**, 2167–2201.

Stubbe, J. & van der Donk, W. A. (1998). Protein radicals in enzyme catalysis. *Chemical Reviews* **98**, 705–762.

Takematsu, K., Williamson, H., Blanco-Rodríguez, A. M., Sokolová, L., Nikolovski, P., Kaiser, J. T., Towrie, M., Clark, I. P., Vlček, A., Winkler, J. R. & Gray, H. B. (2013). Tryptophan-accelerated electron flow across a protein–protein interface. *Journal of the American Chemical Society* **134**, 15515–15525.

Taylor, J. S. (1994). Unraveling the molecular pathway from sunlight to skin cancer. *Accounts of Chemical Research* **27**, 76–82.

Vidal-Limon, A., Aguila, S., Ayala, M., Batista, C. V. & Vazquez-Duhalt, R. (2013). Peroxidase activity stabilization of cytochrome P450(BM3) by rational analysis of intramolecular electron transfer. *Journal of Inorganic Biochemistry* **122**, 18–26.

Warman, A. J., Roitel, O., Neeli, R., Girvan, H. M., Seward, H. E., Murray, S. A., McLean, K. J., Joyce, M. G., Toogood, H., Holt, R. A., Leys, D., Scrutton, N. S. & Munro, A. W. (2005). Flavocytochrome P450BM3: an update on structure and mechanism of a biotechnologically important enzyme. *Biochemical Society Transactions* **33**, 747–753.

Warren, J. J., Ener, M. E., Vlček, A., Winkler, J. R. & Gray, H. B. (2012). Electron hopping through proteins. *Coordination Chemistry Reviews* **256**, 2478–2487.

Warren, J. J., Herrera, N., Hill, M. G., Winkler, J. R. & Gray, H. B. (2013*a*). Electron flow through nitrotyrosinate in *Pseudomonas aeruginosa* azurin. *Journal of the American Chemical Society* **135**, 11151–11158.

Warren, J. J., Winkler, J. R. & Gray, H. B. (2013*b*). Hopping maps for photosynthetic reaction centers. *Coordination Chemistry Reviews* **257**, 165–170.

Whitehouse, C. J. C., Bell, S. G. & Wong, L. L. (2012). P450BM3 (CYP102A1): connecting the dots. *Chemical Society Reviews* **41**, 1218–1260.

Wikström, M. (2012). Active site intermediates in the reduction of O_2 by cytochrome oxidase, and their derivatives. *Biochimica et Biophysica Acta – Bioenergetics* **1817**, 468–475.

Wilson, T. D., Yu, Y. & Lu, Y. (2013). Understanding copper-thiolate containing electron transfer centers by incorporation of unnatural amino acids and the Cu-A center into the type 1 copper protein azurin. *Coordination Chemistry Reviews* **257**, 260–276.

Winkler, J. R. & Gray, H. B. (2014*a*). Electron flow through metalloproteins. *Chemical Reviews* **114**, 3369–3380.

Winkler, J. R. & Gray, H. B. (2014*b*). Long-range electron tunneling. *Journal of the American Chemical Society* **136**, 2930–2939.

Woiczikowski, P. B., Steinbrecher, T., Kubař, T. & Elstner, M. (2011). Nonadiabatic QM/MM simulations of fast charge transfer in *Escherichia coli* DNA photolyase. *Journal of Physical Chemistry B* **115**, 9846–9863.

Worsdorfer, B., Conner, D. A., Yokoyama, K., Livada, J., Seyedsayamdost, M., Jiang, W., Silakov, A., Stubbe, J., Bollinger, J. M. & Krebs, C. (2013). Function of the Diiron Cluster of *Escherichia coli* class Ia ribonucleotide reductase in proton-coupled electron transfer. *Journal of the American Chemical Society* **135**, 8585–8593.

Yokoyama, K., Smith, A. A., Corzilius, B., Griffin, R. G. & Stubbe, J. (2011). Equilibration of tyrosyl radicals (Y-356$^{\bullet}$, Y-731$^{\bullet}$, Y-730$^{\bullet}$) in the radical propagation pathway of the *Escherichia coli* class Ia ribonucleotide reductase. *Journal of the American Chemical Society* **133**, 18420–18432.

Yu, M. A., Egawa, T., Shinzawa-Itoh, K., Yoshikawa, S., Guallar, V., Yeh, S. R., Rousseau, D. L. & Gerfen, G. J. (2012). Two tyrosyl radicals stabilize high oxidation states in cytochrome *c* oxidase for efficient energy conservation and proton translocation. *Journal of the American Chemical Society* **134**, 4753–4761.

Yu, M. A., Egawa, T., Shinzawa-Itoh, K., Yoshikawa, S., Yeh, S. R., Rousseau, D. L. & Gerfen, G. J. (2011). Radical formation in cytochrome *c* oxidase. *Biochimica et Biophysica Acta – Bioenergetics* **1807**, 1295–1304.

Yukl, E. T., Liu, F. G., Krzystek, J., Shin, S., Jensen, L. M. R., Davidson, V. L., Wilmot, C. M. & Liu, A. M. (2013). Diradical intermediate within the context of tryptophan tryptophylquinone biosynthesis. *Proceedings of the National Academy of Sciences of the United States of America* **110**, 4569–4573.

https://doi.org/10.1017/S0033583515000062 Published online by Cambridge University Press